The effect of raft lipid depletion on microvilli formation in MDCK cells, visualized by atomic force microscopy

Kate Poole[a,b,*], Doris Meder[b], Kai Simons[b], Daniel Müller[a]

[a] *BioTechnological Center, University of Technology Dresden, D-01307 Dresden, Germany*
[b] *Max Planck Institute for Molecular and Cell Biology and Genetics, Pfotenhauerstrasse 108, D-01307 Dresden, Germany*

Received 13 February 2004; revised 25 March 2004; accepted 29 March 2004

First published online 15 April 2004

Edited by Amy McGough

Abstract We have investigated whether raft lipids of Madin–Darby canine kidney (MDCK) cells play any role in microvilli maintenance using a combination of atomic force microscopy (AFM) and laser scanning confocal microscopy. MDCK cells were treated to reduce the amount of sphingolipids, cholesterol, or both and subsequently imaged, in buffer solution, using AFM. It was observed that inhibition of either sphingolipid or cholesterol biosynthesis led to a reduction in the number of microvilli on the surface of MDCK cells. However, this effect was not uniform across the monolayer, with some cells resembling those in untreated controls. The subsequent extraction of cholesterol from cells grown in the presence of inhibitors led to a further reduction in microvilli on the surface of the cells and, in some cases, resulted in monolayers devoid of full length microvilli. Significantly, smaller spikes were observed on the surface of the smoother cells.

Keywords: Madin–Darby canine kidney; Microvillus; Raft lipid; Atomic force microscopy; Laser scanning confocal microscopy

1. Introduction

The structure and composition of the plasma membrane of Madin–Darby canine kidney (MDCK) cells is not homogeneous and can be described in terms of domains and sub-domains [1]. The formation of tight junctions between cells assembled in a confluent monolayer leads to their polarization into apical and basolateral domains [2,3]. In comparison with the basolateral plasma membrane domain, the apical membrane is enriched in glyco-sphingolipids, which are postulated to form dynamic assemblies with membrane cholesterol in the exoplasmic leaflet, known as lipid rafts [1,4].

In model membranes containing a binary mixture of lipids, sphingomyelin and phosphatidyl choline, lipid–lipid interactions can lead to phase separation and the formation of distinct domains. The long saturated hydrocarbon chains of sphingomyelin allow tight packing, forming a gel-like phase surrounded by a fluid phase, in which the unsaturated phosphatidyl choline lipid is loosely packed. The addition of cholesterol to such model membranes results in a liquid ordered phase, in place of the gel phase, in which the sphingomyelin saturated hydrocarbon chains are still tightly packed but exhibit a higher degree of lateral movement [5,6].

The lipid raft hypothesis proposes that, in the exoplasmic leaflet of the lipid bilayer, dynamic assemblies of cholesterol and sphingolipids form [3], which are organized in a liquid ordered state, similar to that found in model membranes [7]. One important function of such rafts is to allow lateral sorting of different proteins within the membrane [8–10], based on varying affinities of particular proteins for lipid rafts [11–13]. Such a mechanism allows for the partitioning of proteins into distinct micro-environments, enabling polarization [14], localized modification of phosphorylation state [10,15], or clustering [16]. The disruption of the liquid ordered phase, by removal of cholesterol, leads to increased solubility of raft-associated proteins in Triton X-100 [17].

Structurally, the organization of the apical surface of MDCK cells can be described in terms of microvillar and planar sub-domains [18]. Microvilli formation requires the reorganization of cytoskeletal elements, i.e., actin bundling. It is possible that lateral organization of plasma membrane elements influences the vertical interaction between membrane components and the sub-membranous actin cytoskeleton. There is evidence that, in the Jurkat T cell line, actin accumulates in raft-like membrane patches in a process requiring tyrosine phosphorylation. In contrast, actin does not accumulate in regions underlying non-raft membrane regions [15]. Furthermore, raft domains have been reported to be preferred sites for membrane-linked actin polymerization requiring tyrosine signaling and local synthesis of phosphoinositol(4,5)bis-phosphate ($PI(4,5)P_2$) in the cytosolic leaflet [19]. The extraction of cholesterol from the plasma membrane has been shown to reduce the number of microvilli on the surface of MDCK cells [20]. However, an association between lipid rafts and microvilli formation is not clear, since the raft-associated placental alkaline phosphatase (PLAP) does not co-localize with microvilli, being enriched, instead, on the planar regions of the cell [21].

It has previously been shown that the abundance of microvilli on the surface of MDCK cells is affected by treatment with methyl-β-cyclodextrin (MBCD) [20]. Here, we have carefully investigated the effect of raft lipid depletion on microvilli formation, by atomic force microscopy (AFM). The

* Corresponding author. Fax: +49-351-210-2020.
E-mail address: poole@mpi-cbg.de (K. Poole).

Abbreviations: AFM, atomic force microscopy; MBCD, methyl-β-cyclodextrin; MDCK, Madin–Darby canine kidney

0014-5793/$22.00
doi:10.1016/j.febslet.2004.03.095

AFM allows complex biological systems to be observed under physiological conditions [22]. It operates in buffer solution at ambient temperatures and can image biological surfaces with an outstanding signal-to-noise ratio. It, therefore, represents the only microscopy technique that allows observation of biological objects across dimensions, from tissues [23] to cells [24–26] to single proteins and their detailed sub-structures [27]. As a surface technique, the AFM provides a nearly perfect tool to study cellular membranes in detail. Hence, the AFM is particularly suitable for the study of the compartmentalization of cell surfaces. The sensitivity and signal-to-noise ratio of the AFM has enabled the imaging of certain single membrane proteins and their sub-structures [27]. However, single proteins on the cell surface have never been resolved. Several reasons may account for this, namely, the relative flexibility and mobility of the cellular membrane, and the presence of a glycocalyx, which consists of highly branched sugar residues that may extend above the surface of the cell, obscuring underlying proteins and protein complexes. However, we have used AFM to obtain high-resolution images of complex cell surface structures, i.e., microvilli, and to investigate the effect of lipid depletion on such structures.

A number of approaches were taken to disrupt membrane organization, by inhibiting sphingolipid and cholesterol biosynthesis in addition to cholesterol extraction. In this way, we have been able to show that raft lipids are necessary for the formation of microvillar structures on the MDCK cell surface.

2. Materials and methods

2.1. Cell culture

MDCK type II cells, obtained from the American Type Tissue Collection, Rockville, MD/USA, were maintained in minimal essential medium (MEM) with Earle's salts (Gibco-BRL) supplemented with 2 mM L-glutamine, penicillin–streptomycin and 5% FCS (PAA) at 37 °C in a 95% air/5% CO_2 humidified incubator. Confluent cells were released from the plastic using trypsin-EDTA (Invitrogen). Routine cultures were fed with fresh medium every other day and routinely checked for mycoplasma contamination.

2.2. Manipulation of raft lipids

To extract cholesterol, MDCK cells were plated on 12-mm round, glass coverslips and grown to confluence. Monolayers were then incubated, for 30 or 60 min, in freshly prepared MBCD (10 mM) in CO_2 independent media, without serum, at room temperature. To inhibit cholesterol synthesis, cells were allowed to attach overnight. After attachment, cells were cultivated in MEM containing 250 μM mevalonate and 4 μM lovastatin for 48 h. For the inhibition of glycosphingolipid synthesis, cells were allowed to attach overnight and were then cultivated in MEM containing either 25 μg/ml fumonisin or 10 μM myriocin for 48 h. Cells were stained with Rhodamine 123 (10 μg/ml, 10 min) to confirm that the treatment with inhibitors was not lethal. For lipid analysis, lipids from roughly 2×10^6 cells were extracted according to Folch et al. [28]. Lipids were resolved by two sequential thin layer chromatography (TLC) runs, first in chloroform:methanol:water (65:35:8), second in hexane:ethylacetate (5:1), stained with sulfuric acid spraying and quantified using Image Gauge V3.3 (Fuji, Japan).

2.3. Atomic force microscopy

AFM imaging was conducted using a NanoWizard (JPK Instruments, Berlin, Germany), mounted on a Zeiss Axiovert 200M (Carl Zeiss, Goettingen, Germany). Before imaging, cells were fixed using 2% glutaraldehyde in PBS, for 15 min. Imaging of cells was performed in PBS containing 1 mM $CaCl_2$ and 0.5 mM $MgCl_2$, at room temperature. To compensate for evaporation, the buffer was exchanged at regular intervals of 1 h. Topographs were taken in low force contact mode using 200-μm long V-shaped cantilevers, with nominal spring constants of 0.06 N/m. The force applied to the cantilever was adjusted manually to about 50 pN. This force was just sufficient for the stylus of the cantilever to remain in contact with the surface during the scanning process. To optimize image quality, the scan rate was kept between 0.3 and 0.6 Hz. Topographs and error signal images were collected, simultaneously, in both the trace and retrace directions.

2.4. Confocal microscopy

Cells were grown on 22-mm coverslips and fixed with 2% glutaraldehyde for 30 s, followed by 3% paraformaldehyde for 20 min. The cell membrane was permeabilized with Triton X-100, 0.5% for 60 s, and the F-actin labeled with Alexa 488-phalloidin (Molecular Probes) diluted 1:1000 in PBS from manufacturers suggested stock. Cells were then imaged in PBS with an LSM 510 Meta (Carl Zeiss, Jena, Germany) using a 63×1.2 NA water immersion objective.

2.5. Image analysis

In some cases, as noted in the figure legend, particular images were processed to reveal edges, using the soebel edge detection function of the JPK image processing software (JPK Instruments, Berlin, Germany). Microvilli heights were measured, taking a cross-section parallel to the scan direction, and measuring the half-maximal height of each structure. Microvilli heights were determined from topographs taken with a scan size of 20 μm × 20 μm (512 × 512 pixels). To measure the height of the significantly smaller protrusions on treated cells, measurements were taken using cross-sections of topographs of scan size 5 μm × 5 μm. To enhance visualization of microvilli, the AFM image background, calculated by image erosion, was subtracted from the original using MATLAB (Math Works, Massachusetts, USA).

3. Results

In constant force mode, there is a constant mechanical interaction between the stylus of the AFM and the cell sample. The application of too high forces during the scanning process can thus distort the surface, making it impossible to reproducibly visualize details. When MDCK cells are scanned at too high forces (2 nN and above), the microvilli are not resolved and the surface appears smooth and fuzzy [25]. Careful imaging at low forces (<300 pN), however, reveals structures, most likely corresponding to microvilli, on the surface [26].

Cells imaged by AFM were fixed with glutaraldehyde or paraformaldehyde for two reasons. First, the scanning process takes about 30 min to record a topograph. Thus, the surface of the MDCK cells had to be trapped in one condition. Second, fixed cells allow for higher resolution of the AFM topographs, in comparison with the softer surface of living cells. After fixing, cells were imaged at low force and slow scan speed to reveal high resolution topographs with reproducible quality. Fig. 1 shows the reticulated surface structure of untreated MDCK cells. Although the cell surfaces were imaged using low-force contact mode, the microvilli were bent slightly in the scanning direction of the AFM stylus. The flexible projections, corresponding to microvilli, covered the entire apical surface of MCDK cells. Analysis of the AFM topographs revealed that the height of these protrusions was variable (Table 1). The boundaries between cells were clearly visualized, being somewhat raised above the surface. However, these cell boundaries were not uniform in neither height nor width. On some cells, a single, large protrusion was also observed near cell boundaries (1.1 ± 0.3 μm in height). The exact dimensions of such protrusions could not be distinguished as it is clear from their pyramidal shape that the AFM tip has influenced the resulting image. These larger protrusions have previously been visual-

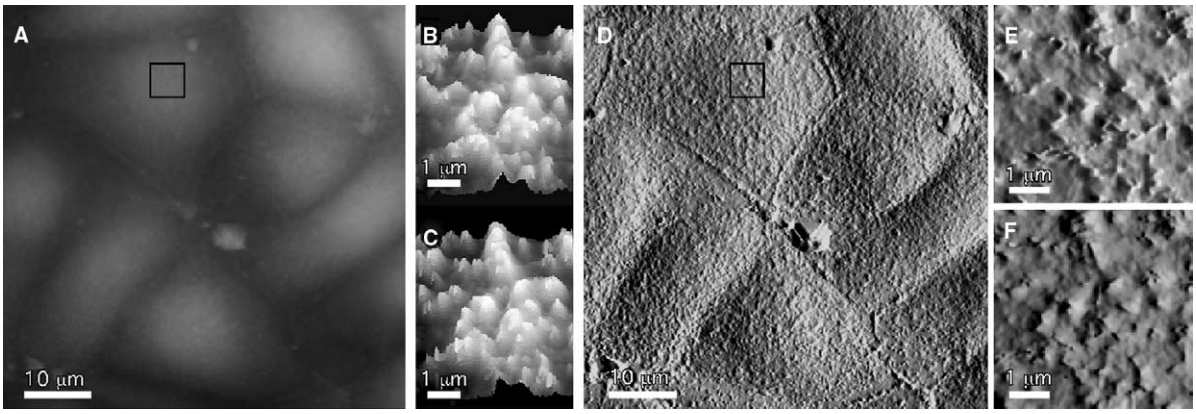

Fig. 1. MDCK monolayers expose microvilli clusters on their apical surface. AFM topography of cells within the monolayer reveals that their surface is covered by flexible protrusions (A, height range 5.7–11.9 μm). Electronic zooms of the topographs, recorded in trace (B) and retrace (C) scan directions, show slight displacement of the flexible structures on the surface of the cell, due to the mechanical interaction of the tip with the sample. Processed AFM topographs revealed edges and give a clearer impression of the protrusions (D). Higher magnification images of the cell surface, again processed to reveal edges, are presented in trace (E) and retrace (F) scanning directions. Scale bars: A,D = 10 μm; B,C,E,F = 1 μm.

Table 1
Prevalence and height of microvilli on the surface of MDCK cells

Treatment	Normal microvilli density		Reduced microvilli density		Depleted microvilli density	
	%	Height (nm)	%	Height (nm)	%	Height (nm)
Control	100	74–496 (183 ± 79)	0	–	0	–
MBCD	100	51–428 (196 ± 83)	0	–	0	–
Fumonisin	4	70–376 (170 ± 64)	87	67–384 (173 ± 65)	9	6–102 (40 ± 26)
Myriocin	90	60–377 (170 ± 61)	10	80–352 (180 ± 66)	0	–
Myriocin/MBCD	0	–	18	52–460 (163 ± 72)	82	10–95 (35 ± 17)
myr/mev/lov	66	70–396 (160 ± 61)	34	34–395 (165 ± 55)	0	–
myr/mev/lov/MBCD	0	–	24	69–327 (159 ± 60)	76	5–97 (37 ± 17)

Percentages represent cells within the monolayer classed as having normal (resembling untreated controls, surface covered with microvilli), reduced (noticeable increase in planar regions and decrease in microvilli) or depleted microvilli (few or no microvilli) density ($n > 50$). Heights of flexible protrusions were measured, revealing a high variability in heights of protrusions on each cell, presented as the range of heights and the mean and standard deviation ($n > 100$).

ized by AFM, in a study where microvilli were not evident in the topographs, probably due to too high scanning forces [25].

In order to confirm that the protrusions imaged on the surface of the MDCK cells were actin-based microvilli, AFM was combined with laser-scanning confocal microscopy of cells in which the actin was fluorescently labeled with Alexa-488 phalloidin. A comparison of the images generated by each of these microscopy techniques shows that the protrusions on the surface of the MDCK cells can be correlated to actin-based structures (Fig. 2). There is some discrepancy between the protrusions in the AFM image and the actin bundles in the confocal image. This is probably due to the slight displacement of protrusions in the scan direction by the tip during the AFM scanning process.

MBCD has previously been shown to rapidly decrease the amount of cholesterol in MDCK monolayers, thereby

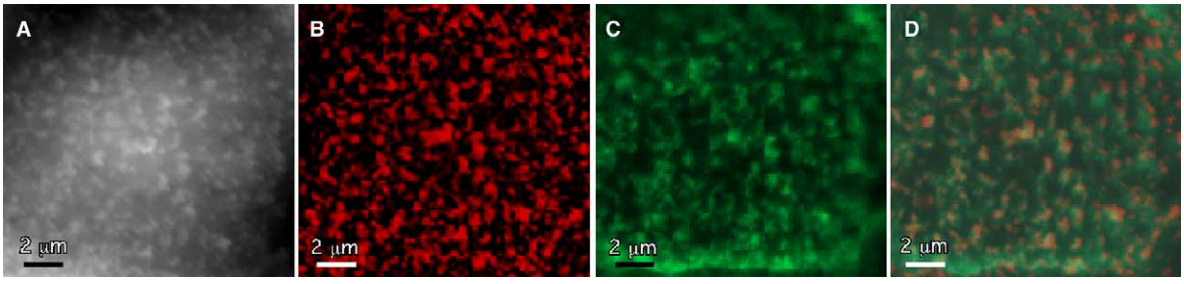

Fig. 2. Correlation of laser scanning confocal microscopy of fluorescently labeled actin confirms that the protrusions imaged using AFM are actin-based microvilli. The visualization of protrusions on the surface, as imaged in a topograph of a single MDCK cell (A), was enhanced by treating the curvature of the cell as background and subtracting it from the original image (B). Phalloidin-labeled actin imaged at the surface of the same cell, using laser scanning confocal microscopy (C). The processed AFM topograph (B, red) and confocal image (C, green) were merged (D). The microvilli in the AFM topograph are slightly displaced in the scan direction. Scale bars: A,B = 2 μm.

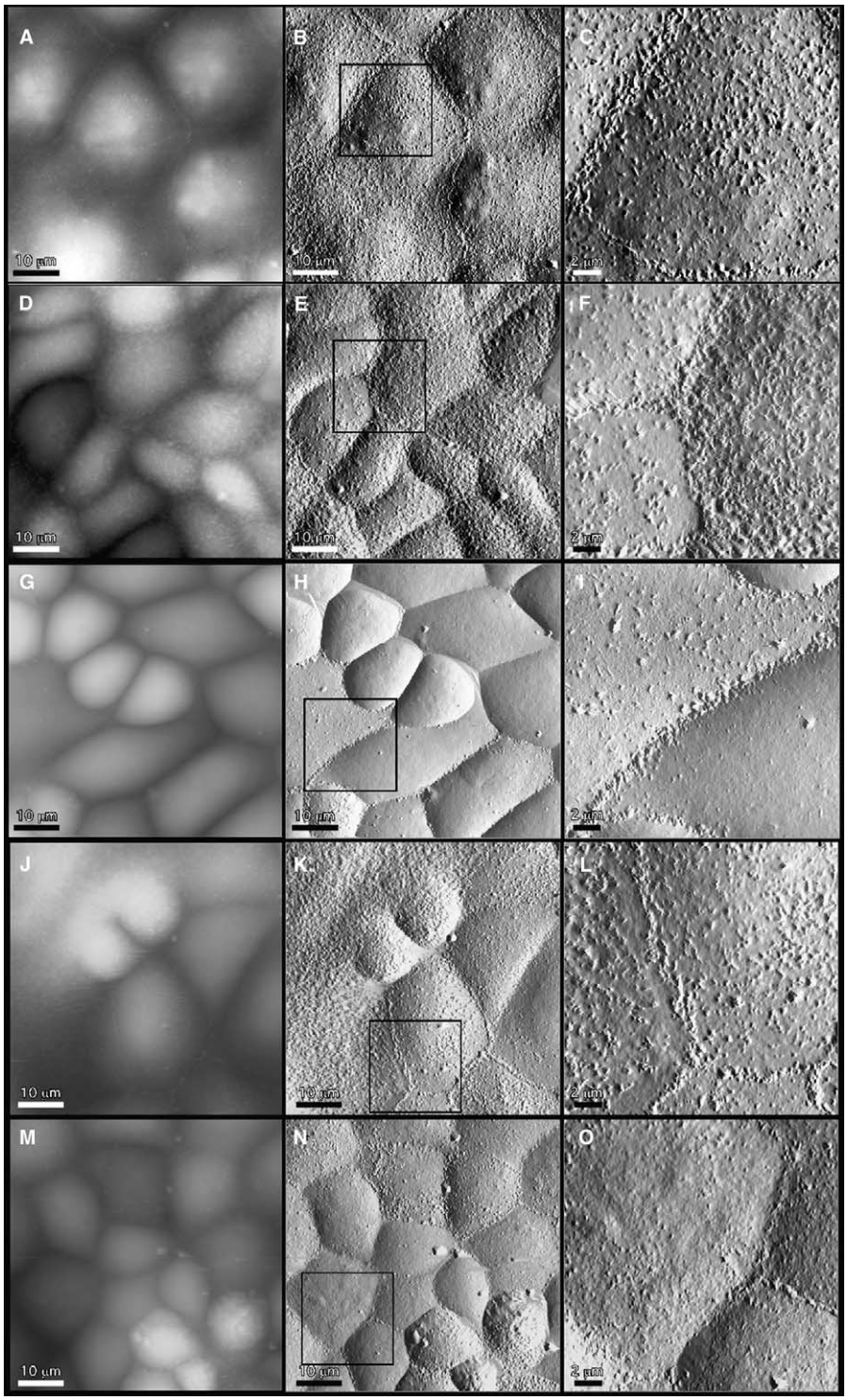

Fig. 3. Treatment of MDCK cells to inhibit lipid raft formation decreases the number of microvilli, AFM topographs of MDCK monolayers treated for 48 h with fumonisin (A, height range 4.8–10.4 μm), myriocin (D, height range 5.7–13.1 μm) or myriocin, mevalonate and lovastatin (J, height range 4.1–13.0 μm). Some cells within the monolayer show a reduction in the proportion of the surface covered in microvilli. After processing to reveal edges, the contrast between microvillar and planar regions is more easily distinguished (B,E,K). Processed images in (C,F,L) correspond to the regions marked in (B,E,K). MBCD was used to extract cholesterol, for 30 min, from cells grown in the presence of myriocin (G, height range 2.5–11.0 μm) or from cells grown in the presence of myriocin, mevalonate and lovastatin (M, height range 4.1–12.6 μm) for 2 days. The corresponding processed images (H and N) reveal the smooth surface of cells, largely devoid of microvilli. (I and O), cell surface recorded at higher magnification, corresponding to the regions marked in (H and N). Scale bars: A,B,D,E,G,H,J,K,M,N = 10 μm; C,F,I,L,O = 2 μm.

reducing the number of microvilli on the surface of the MDCK cells [20]. This was determined by transmission electron microscopy of cell sections. As a surface sensitive technique, AFM allows direct imaging of microvilli distribution on the cell surface. To test whether raft lipids play any role in microvilli structure, we depleted cholesterol by addition of

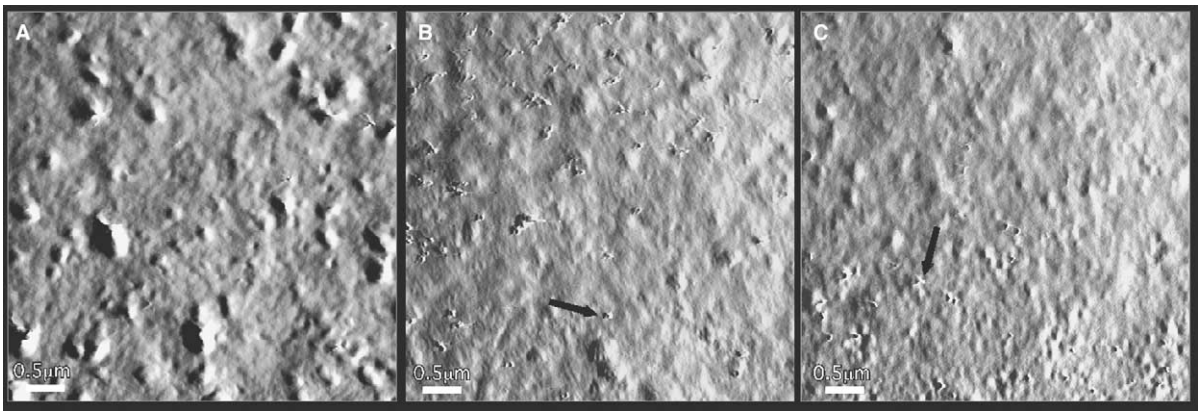

Fig. 4. Higher magnification AFM topographs of cells lacking microvilli reveals the presence of significantly smaller spikes. Topographic data, processed to reveal edges of the surface of cells treated with fumonisin (A), myriocin and MBCD (B), or myriocin, mevalonate, lovastatin and MBCD (C) revealed small, flexible protrusions (closed arrows). The shape of these protrusions cannot be determined due to the influence of tip structure on the image. Scale bars: 500 nm.

MBCD to MDCK cell monolayers, for 30 or 60 min. In our experiments, the distribution of microvilli on the cell surface of the monolayer did not change significantly upon exposure to MBCD (data not shown). In addition, the average height of the microvilli was not significantly different to that measured in the untreated control cells (Table 1).

It is known that cholesterol depletion is insufficient for lipid raft disassembly in model membranes [29]. To further disrupt membrane organization, we depleted glycosphingolipids by growing the cells in the presence of either fumonisin B1 or myriocin. Fumonisin B1 is a fungal mycotoxin that inhibits ceramide-synthetase activity, blocking the final step of ceramide synthesis and, hence, sphingolipid biosynthesis [30]. Myriocin inhibits serine-palmitoyl transferase, which mediates the first step in sphingolipid biosynthesis. Both drugs reduced the cellular amounts of glucosylceramide (GlcCer), the major glycosphingolipid in MDCK cells, by more than 90%, as determined by TLC. Monolayers grown in the presence of fumonisin B1 for 48 h contained cells with decreased density of microvilli on the surface, whilst other cells within the monolayer did not differ significantly in surface structure from the untreated control cells (Fig. 3). Likewise, the effect on the surface structure of cells grown in the presence of myriocin was not uniform. However, the size of the microvilli on these cells, regardless of microvilli density, was not significantly different, when compared with the untreated control (Table 1). Hence, a reduction in sphingolipids leads to a partial reduction in the density of microvilli distribution, but not the size of individual microvilli.

We reasoned that the most drastic influence on membrane organization and thus on surface structure should be achieved by combining the treatments to reduce both cholesterol and sphingolipids. To investigate the effect of such a double inhibition, cells were grown in myriocin and then treated with MBCD for 30 min (Fig. 3). Here, the exposure to MBCD reduced the amount of microvilli. TLC analysis of the lipid composition of treated cells showed that, in addition to the reduction in GlcCer, total cellular cholesterol levels were reduced by roughly 30%, but since MBCD here acted mostly on the apical plasma membrane, the relative cholesterol depletion in the apical membrane was most likely higher. The growth of cells in the presence of myriocin and lovastatin/mevalonate (to inhibit cholesterol synthesis) had a similar effect on the presence of microvilli to growth in myriocin alone (Fig. 3). The further reduction of cholesterol in these cells, using MBCD, again decreased the number of microvilli on the surface (Fig. 3). As determined by TLC, inhibition of cholesterol synthesis with lovastatin resulted in mobilization of cholesterol esters, but cholesterol levels were only mildly reduced. Only in combination with MBCD could we achieve a depletion of roughly 30% of cellular cholesterol, as seen for the combined myriocin, MBCD treatment.

When cells devoid of microvilli were imaged at a higher magnification (Fig. 4), spikes of variable height were observed protruding from the cell surface (Table 1). Again, the spikes were bent slightly in the direction of the AFM stylus. These spikes were significantly smaller than those assigned as microvilli of untreated cells (Fig. 1). If present in the control monolayers, they were obscured by larger protrusions covering the cell surface. Thus, the depletion of both sterols and sphingolipids led to the loss of microvilli.

4. Discussion

In this work, the effect of raft lipid depletion on the presence of microvilli on MDCK cells has been investigated. AFM imaging, at low forces, low speed and under optimized conditions allowed visualization of surface structures on the apical surface that correspond to microvilli. However, individual microvilli appeared clustered, making correlation of protrusions to a single microvillus difficult. The fact that AFM imaging relies on a mechanical interaction with the sample also results in the bending of flexible surface structures in the scanning direction of the AFM stylus. Consequently, this leads to the underestimation of the height of such structures and the measured height of microvilli appeared to be variable (Table 1). This distribution of microvilli heights would suggest a dynamic process of microvillar growth and subsequent retraction. This is supported by the finding that microvilli formation on the surface of living *Xenopus* kidney epithelial A6 cells has been shown to be a dynamic process, by scanning ion conductance microscopy [31].

Are lipid rafts of the MDCK plasma membrane localized to microvilli? Previous publications do not give a definitive answer to this question. On one hand, a classical marker of lipid rafts, PLAP, does not colocalize with the microvillar regions of the cell surface [21]. In addition, the association of membrane proteins with lipid rafts is usually determined by density flotation after solubilization with Triton X-100 at 4 °C, with raft-associated proteins remaining in the insoluble fraction. A plasma membrane marker that does localize to microvillar regions and whose distribution is cholesterol dependent, prominin, is soluble under these conditions [21,32]. Our results suggest that raft lipids are involved in the formation of microvilli. We observed that the metabolic inhibition of synthesis of raft lipids affects the formation of microvilli on the surface of MDCK cells. Previously, extraction of cholesterol from the plasma membrane, using MBCD, was shown to reduce the density of microvilli [20]. In this study, a reduction of the microvilli density, due to MBCD treatment, was observed only when the cells had been cultured in the presence of inhibitors of either cholesterol or sphingolipid synthesis, before the addition of MBCD. Treatment with metabolic inhibitors, alone, did reduce the number of microvilli on the surface of some cells within the monolayer, whereas other cells remained unaffected (Fig. 3(B, E and K)). Only the inhibition of sphingolipid synthesis, combined with the extraction of cholesterol from the cell, led to a complete loss of microvillar structures (Fig. 3(H and N)).

Although the disruption of biosynthetic pathways may have pleiotropic effects on cell function, the observed reduction in microvilli formation, as a result of the chemical extraction of cholesterol, indicates that the presence of raft lipids in the plasma membrane is critical for the organization of the MDCK cell surface into microvillar and planar regions. One of the organizers of the membrane-cytoskeleton interphase is $PI(4,5)P_2$ which has been shown to accumulate in raft domains [33]. Interestingly, cholesterol depletion has been reported to result in the loss of $PI(4,5)P_2$ from the plasma membrane leading to alterations in the actin cytoskeleton [34]. Something similar might be the reason for our observation of a loss of microvilli, the shape of which is dependent on polymerized actin [35].

5. Conclusions

The inhibition of biosynthesis of either sphingolipids or sphingolipids and cholesterol leads to a reduction in microvilli density. The extraction of cholesterol after the inhibition of lipid biosynthesis leads to the complete loss of microvilli. Together with the previous work [20], our data suggest that raft lipids are essential for microvilli maintenance, possibly by providing the membrane architecture necessary for cytoskeletal organization.

Acknowledgements: The authors thank Lars Kuerschner and Christoph Thiele for help with the lipid analysis and Fedor Severin for constructive comments. This work was supported by the European Union and the State of Saxonia.

References

[1] Simons, K. and Ikonen, E. (1997) Nature 387, 569–572.
[2] van Meer, G., Stelzer, E.H., Wijnaendts-van-Resandt, R.W. and Simons, K. (1987) J. Cell Biol. 105, 1623–1635.
[3] van Meer, G. and Simons, K. (1988) J. Cell. Biochem. 36, 51–58.
[4] Brown, D.A. and London, E. (2000) J. Biol. Chem. 275, 17221–17224.
[5] Ahmed, S.N., Brown, D.A. and London, E. (1997) Biochemistry 36, 10944–10953.
[6] Brown, R.E. (1998) J. Cell Sci. 111 (Pt 1), 1–9.
[7] Brown, D.A. and London, E. (1997) Biochem. Biophys. Res. Commun. 240, 1–7.
[8] Brown, D.A. and Rose, J.K. (1992) Cell 68, 533–544.
[9] Sargiacomo, M., Sudol, M., Tang, Z. and Lisanti, M.P. (1993) J. Cell Biol. 122, 789–807.
[10] Arreaza, G., Melkonian, K.A., LaFevre-Bernt, M. and Brown, D.A. (1994) J. Biol. Chem. 269, 19123–19127.
[11] Schroeder, R., London, E. and Brown, D. (1994) Proc. Natl. Acad. Sci. USA 91, 12130–12134.
[12] Melkonian, K.A., Ostermeyer, A.G., Chen, J.Z., Roth, M.G. and Brown, D.A. (1999) J. Biol. Chem. 274, 3910–3917.
[13] Moffett, S., Brown, D.A. and Linder, M.E. (2000) J. Biol. Chem. 275, 2191–2198.
[14] Pierini, L.M., Eddy, R.J., Fuortes, M., Seveau, S., Casulo, C. and Maxfield, F.R. (2003) J. Biol. Chem. 278, 10831–10841.
[15] Harder, T. and Simons, K. (1999) Eur. J. Immunol. 29, 556–562.
[16] Baron, W., Decker, L., Colognato, H. and ffrench-Constant, C. (2003) Curr. Biol. 13, 151–155.
[17] Schroeder, R.J., Ahmed, S.N., Zhu, Y., London, E. and Brown, D.A. (1998) J. Biol. Chem. 273, 1150–1157.
[18] McAteer, J.A., Dougherty, G.S., Gardner Jr., K.D. and Evan, A.P. (1986) Scan. Electron. Microsc., 1135–11350.
[19] Rozelle, A.L. et al. (2000) Curr. Biol. 10, 311–320.
[20] Francis, S.A., Kelly, J.M., McCormack, J., Rogers, R.A., Lai, J., Schneeberger, E.E. and Lynch, R.D. (1999) Eur. J. Cell. Biol. 78, 473–484.
[21] Roper, K., Corbeil, D. and Huttner, W.B. (2000) Nat. Cell. Biol. 2, 582–592.
[22] Drake, B. et al. (1989) Science 243, 1586–1589.
[23] Lydataki, S., Tsilimbaris, M.K., Lesniewska, E.S., Bron, A. and Pallikaris, I.G. (2004) Methods Mol. Biol. 242, 69–83.
[24] Radmacher, M., Tillamnn, R.W., Fritz, M. and Gaub, H.E. (1992) Science 257, 1900–1905.
[25] Hoh, J.H. and Schoenenberger, C.A. (1994) J. Cell Sci. 107, 1105–1114.
[26] Lesniewska, E., Giocondi, M.C., Vie, V., Finot, E., Goudonnet, J.P. and Le Grimellec, C. (1998) Kidney Int. Suppl. 65, S42–S48.
[27] Muller, D.J., Janovjak, H., Lehto, T., Kuerschner, L. and Anderson, K. (2002) Prog. Biophys. Mol. Biol. 79, 1–43.
[28] Folch, J., Lees, M. and Sloane Stanley, G.H. (1957) J. Biol. Chem. 226, 497–509.
[29] Schuck, S., Honsho, M., Ekroos, K., Shevchenko, A. and Simons, K. (2003) Proc. Natl. Acad. Sci. USA 100, 5795–5800.
[30] Merrill Jr., A.H., van Echten, G., Wang, E. and Sandhoff, K. (1993) J. Biol. Chem. 268, 27299–27306.
[31] Gorelik, J. et al. (2003) Proc. Natl. Acad. Sci. USA 100, 5819–5822.
[32] Corbeil, D., Roper, K., Fargeas, C.A., Joester, A. and Huttner, W.B. (2001) Traffic 2, 82–91.
[33] Laux, T., Fukami, K., Thelen, M., Golub, T., Frey, D. and Caroni, P. (2000) J. Cell Biol. 149, 1455–1472.
[34] Kwik, J., Boyle, S., Fooksman, D., Margolis, L., Sheetz, M.P. and Edidin, M. (2003) Proc. Natl. Acad. Sci. USA 100, 13964–13969.
[35] Mooseker, M.S. (1985) Annu. Rev. Cell. Biol. 1, 209–241.